**HETEROGENEOUS DISTRIBUTION OF CHROMIUM ON MERCURY.** L. R. Nittler[1,*], A. Boujibar[2], E. Crapster-Pregont[3], E. A. Frank[1], T. J. McCoy[4], F. M. McCubbin[5], Richard D. Starr[6,7], K. E. Vander Kaaden[8], A.Vorburger[2,9], S. Z. Weider[1], [1]Department of Terrestrial Magnetism, Carnegie Institution of Washington, Washington, DC 20015, USA, [2]Geophysical Laboratory, Carnegie Institution of Washington, Washington, DC 20015, USA,[3]Department of Earth and Planetary Sciences, American Museum of Natural History, New York, NY 10024, USA, [4]National Museum of Natural History, Smithsonian Institution, Washington, DC 20013, USA, [5]NASA Johnson Space Center, Houston, TX 77058, USA, [6]Physics Department, The Catholic University of America, Washington, DC 20064, USA, [7]Solar System Exploration Division, NASA Goddard Space Flight Center, Greenbelt, MD 20771, USA, [8]Jacobs, NASA JSC, Houston, TX 77058, USA, [9]Physics Institute, University of Bern, Bern, Switzerland. *E-mail: lnittler@ciw.edu.

**Introduction:** Measurements made with geochemical instruments on the MESSENGER spacecraft revealed that Mercury's crust is surprisingly rich in volatile elements, including S, Na, K, Cl, and C, and that it is enriched in Mg and depleted in Al, Ca, and Fe, relative to other terrestrial planets [1–5]. Geochemical maps also indicated the presence of a number of distinct geochemical terranes [6, 7]. The MESSENGER X-ray Spectrometer (XRS) detected X-ray fluorescence, induced by incident solar X-rays, from the top ~10s of μm of Mercury's surface. Like Fe, Cr was only detectable by XRS during large solar flares [5]. However, accurate Cr measurements are more susceptible to systematic errors than other elements measured by the XRS [3, 5]. Therefore, to date, Cr data have been published for only 11 XRS measurements [5], but we have recently [8] derived a map of Cr/Si across Mercury's surface. This map is based on data acquired through the complete MESSENGER mission and reveals clear spatial heterogeneity in Cr.

**Methods:** Following previous methods [5,9], we combined analyses of 133 XRS spectra, selected because they had non-zero derived Cr abundances and did not exhibit anomalously high detector backgrounds at high energy, to produce our Cr/Si map [8]. Data were empirically corrected for a phase-angle effect [5,8]. Following this correction, we calculate the global average Cr/Si as 0.003 (~800 ppm Cr), but there is at least a factor of two systematic uncertainty in absolute Cr/Si values. Relative differences between mapped Cr/Si values are much more robust.

**Results and Discussion:** Our Cr/Si map is compared to an XRS-derived Mg/Al ratio map [5] in the Figure. Coverage in the northern hemisphere is sparse for Cr/Si and spatial resolution is poor in the south, but the map includes multiple resolved measurements across the High-Magnesium Region (HMR) and Caloris Basin (CB) geochemical terranes. The HMR, which is also enriched in Mg, S, Ca, and Fe, and depleted in Al, has a clear enrichment in Cr compared with the global average (Cr/Si~0.0054, 1.8±0.4×average). Conversely, the CB interior plains, which exhibit the lowest Mg/Al on the planet, have a low Cr/Si ratio, with an average value of 0.0016, 0.54±0.11 times the average. Thus, Cr on Mercury correlates with Mg, S, Ca, and Fe, and anti-correlates with Al, at least in large geochemical terranes.

Based on its surface Fe and S composition, Mercury is inferred to have formed under highly reducing conditions, e.g., oxygen fugacity ($fO_2$) of 3 to 7 log units below the iron-wüstite buffer [10-12]. Under these conditions, Cr is expected to be present primarily in sulfides. Moreover, because the valence state of Cr depends on $fO_2$ [13], the new Cr data may provide additional constraints on Mercury's oxidation state [8, 14].

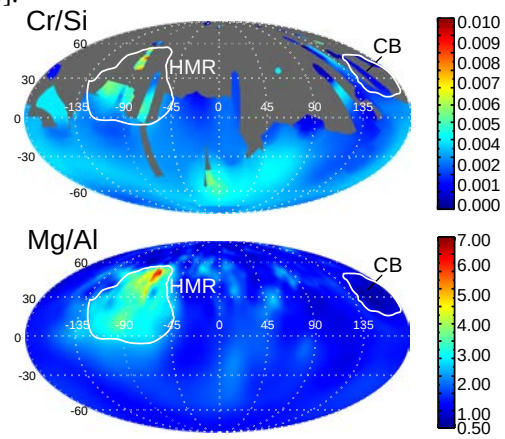


**References:** [1] Nittler L. R., et al. (in press) in: Mercury: The view after MESSENGER, Cambridge University Press, Cambridge. [2] Peplowski P. N., et al. (2011) *Science, 333,* 1850–1852. [3] Nittler L. R., et al. (2011) *Science, 333,* 1847–1850. [4] Peplowski P. N., et al. (2014) *Icarus, 228,* 86–95. [5] Weider S. Z., et al. (2014) *Icarus, 235,* 170–186. [6] Peplowski P. N., et al. (2015) *Icarus, 253,* 346–363. [7] Weider S. Z., et al. (2015) *EPSL, 416,* 109–120. [8] Nittler L. R., et al. (2018) *LPS 49,* Abstract #2070. [9] Nittler L. R., et al. (2016) *LPS, 47,* Abstract #1237. [10] McCubbin F. M., et al. (2012) *GRL,* 39, L09202. [11] Zolotov M. Y., et al. (2013) *JGR (Plan.)* 118, 138–146. [12] Namur O., et al. (2016) *EPSL,* 448, 102–114. [13] Bell A. S., et al. (2014) *Am. Min., 99,* 1404-1412. [14] Boujibar, A., et al. (2018), this meeting.